These estimates are consistent with earlier back-calculation estimates based on AIDS incidence data through mid-1987 [see P. S. Rosenberg, R. J. Biggar, J. J. Goedert, M. H. Gail, *Am. J. Epidemiol.* **133**, 276 (1991)].
25. The analysis of the heterosexual transmission group excludes individuals born in pattern II countries, defined as areas of central, eastern, and southern Africa and some Caribbean countries [Centers for Disease Control, *Morb. Mortal. Wkly. Rept.* **37**, 294 (1988)].
26. The infection rate estimates are sensitive to both the location and shape of the incubation period distribution. For example, if the stage-specific hazards are scaled so that the median incubation period is 9 years instead of 10 years, the estimated cumulative number of infections is 15% lower, although the shape of the infection curve is similar to Fig. 2. See also P. S. Rosenberg and M. H. Gail, *Ann. Epidemiol.* **1**, 105 (1990); J. Taylor, *Stat. Med.* **8**, 45 (1989); J. Hyman and E. Stanley, *Math. Biosci.* **90**, 415 (1988).
27. The back-calculation results on which Fig. 2 is based suggest that 110,000 individuals had fewer than 200 $CD4^+$ cells and did not have an AIDS diagnosis on 1 July 1987. If it is assumed that 20% of these eligible patients enter treatment each year beginning 1 July 1987, then about 11,000 were in treatment in the beginning of 1988. For estimates from drug surveillance studies, see E. Andrews, T. Creagh-Kirk, K. Pattishell, H. Tilson, *J. AIDS* **3**, 460 (1990).
28. R. Brookmeyer and A. Damiano, *Stat. Med.* **8**, 23 (1989); P. S. Rosenberg and M. H. Gail, *Appl. Stat.* **40**, 269 (1991).
29. J. F. Brundage *et al.*, *J. AIDS* **3**, 92 (1990).
30. B. A. Larder, G. Darby, D. D. Richman, *Science* **243**, 1731 (1989).
31. Centers for Disease Control, *Morb. Mortal. Wkly. Rept.* **39** (no. 7), 112 (1990).
32. M. Segal and P. Bacchetti, *J. AIDS* **3**, 832 (1990).
33. L. McKusick, W. Horstman, T. Coates, *Am. J. Publ. Health* **75**, 493 (1987); J. Pickering *et al.*, *Math. Model.* **7**, 661 (1986).
34. T. J. Dondero, M. St. Louis, J. Anderson, L. Petersen, M. Pappaiognou, paper presented at the Fifth International Conference on AIDS, Montreal, 4 to 9 June 1989 (International Development Research Centre, Ottawa, 1989), abstract, p. 45
35. H. W. Hethcote and J. A. Yorke, *Gonorrhea Transmission Dynamics and Control* (Springer-Verlag, Heidelberg, 1984).
36. M. H. Gail, D. Preston, S. Piantadosi, *Stat. Med.* **8**, 59 (1989).
37. J. G. McNeil *et al.*, *N. Engl. J. Med.* **320**, 1581 (1989).
38. J. F. Brundage *et al.*, *J. AIDS* **3**, 1168 (1990).
39. Ranges for projected AIDS incidence account for future infection rates as high as 90,000 per year for all cases; 30,000 per year for each of the following groups: homosexuals, intravenous drug users, and heterosexuals; and 10,000 per year for homosexuals who use intravenous drugs. All lower ranges account for infection rates as low as 0 per year.
40. F. O'Sullivan, B. S. Yandell, W. J. Raynor, *J. Am. Stat. Assoc.* **81**, 96 (1986). Smoothing parameter in Fig. 2 was 6.25×10^{-8}. Smoothing parameters in Fig. 3 for homosexuals, intravenous drug users, homosexuals who use intravenous drugs and heterosexuals were 1.25×10^{-7}, 1.75×10^{-7}, 2.0×10^{-7}, and 1.0×10^{-7}, respectively.
41. Treatment use phased in according to an exponential distribution; among homosexuals, beginning in mid-1987 at a rate of 0.3/year; among intravenous drug users and heterosexuals, beginning in 1988 at a rate of 0.05 per year; among homosexuals who use intravenous drugs, beginning in 1988 at a rate of 0.1 per year. Rates suggested by drug surveillance studies (*12*).
42. The author gratefully acknowledges many helpful discussions with R. Fox, J. Curran, M. H. Gail, T. Green, J. Karon, J. Liao, P. S. Rosenberg, and S. Zeger; P. Hubbard for manuscript preparation, and the support of PHS grant CA-48723 awarded by the National Cancer Institute.

Celestial Mechanics on a Microscopic Scale

T. UZER, DAVID FARRELLY,* JOHN A. MILLIGAN,* PAUL E. RAINES, JOEL P. SKELTON

Classical and semiclassical methods are unrivaled in providing an intuitive and computationally tractable approach to the study of atomic, molecular, and nuclear dynamics. An important advantage of such methods is their ability to uncover in a single picture underlying structures that may be hard to extract from the profusion of data supplied by detailed quantum calculations. Modern trends in semiclassical mechanics are described, particularly the combination of group theoretical methods with techniques of nonlinear dynamics. Application is made to intramolecular energy transfer and to the electronic structure of atomic Rydberg states in external electric and magnetic fields.

THE POPULAR IMAGE OF THE ATOM AS A MINIATURE SOLAR system stems from the experiments of Rutherford and the old quantum theory of Niels Bohr. This theory is described in Max Born's book *Mechanics of the Atom* and is based on the assumption that the laws of classical mechanics apply equally to electrons and planets (*1, 2*). Within months of the appearance of Born's book in 1925, however, a dramatic revolution in physics occurred and the old quantum theory was ousted by the new quantum mechanics of Schrödinger and Heisenberg. As a result, attention in atomic and molecular physics shifted away from classical mechanics, which was thought by many to be a complete and closed field. The analogy between the structure of the atom and that of the solar system seemed invalid, and classical mechanics became the domain of the astronomer. However, new developments within the last two decades have spurred a remarkable revival of interest in classical mechanics (*3*). The implications extend well beyond astronomy, and much present-day research in classical mechanics is being performed in the context of microscopic dynamics. This confluence of interests between atomic and molecular physicists and astronomers is proving beneficial to the study of both classical and quantum systems, as will be illustrated in this article.

The fundamental connection between classical and quantum mechanics has fascinated physicists ever since the discovery of quantum theory (*3–6*), with the most interesting questions relating to the regime where quantum and classical behavior start to overlap. Classical mechanics is an asymptotic limit of quantum mechanics valid when Planck's constant h is small in comparison to relevant system parameters. Although quantum mechanics provides a correct description of nature, it does not hold the intuitive appeal of classical theories, which are also easier to implement: the challenge, therefore, is to understand when the asymptotic classical behavior sets in. Unexpectedly, classical methods many times work rather well in regimes that appear to be removed from the formal asymptotic limit; it is apparent that the uncertainty principle has vanishing impact on the dynamics of a galaxy, but it might seem surprising that interesting behavior of quantum systems can often be described with the use of classical methods. Much of the analysis in molecular vibrational and rotational spectroscopy, for example, is performed using an essentially classical normal mode analysis, which provides a good picture of the dynamics (*7*).

T. Uzer, P. E. Raines, and J. P. Skelton are in the School of Physics, Georgia Institute of Technology, Atlanta, GA 30332. D. Farrelly and J. A. Milligan are in the Department of Chemistry and Biochemistry, University of California, Los Angeles, CA 90024.

*Present address: Department of Chemistry and Biochemistry, Utah State University, Logan, UT 84322.

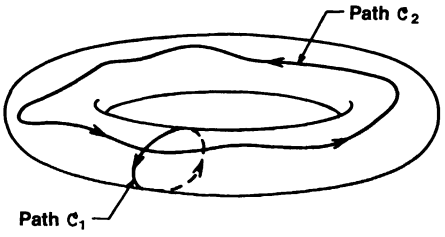

Fig. 1. A 2-D torus arising in the quantization of a 2-D integrable Hamiltonian based on Eq. 2. This manifold is embedded in a 4-D phase-space and two possible quantization paths $\mathcal{C}_1$ and $\mathcal{C}_2$ are shown. Adapted from (*50*).

The revival of interest in classical mechanics has been due in large part to the development of high-speed computers, which have made possible the simulation of classical (as well as quantum) systems. A surprising and fairly recent discovery stemming from these simulations is the phenomenon of classical chaos (*3, 8*). Two prominent examples of chaotic dynamics from astronomy and astrophysics are the tumbling of Saturn's moon Hyperion and the dynamics of the Giant Dark Spot on Neptune (*9*). However, chaos exists in systems as simple as a one-dimensional (1-D) pendulum subjected to a periodic perturbation (*10*). Although the motion of chaotic (technically called nonintegrable) Hamiltonian systems is deterministic, the long-time evolution is, in practice, unpredictable (*3, 4, 9, 11*) because of the extreme sensitivity of the dynamics to initial conditions. These developments in classical mechanics indicate that the relation between classical and quantum mechanics is intricate. Understandably, much attention has been directed toward determining the possible ramifications of chaos for quantum theory (*3–6*). Even in the absence of a clear-cut connection between classical chaos and quantum mechanics, much can be learned from an application of classical and semiclassical methods to microscopic dynamical systems.

Experimental advances have made it possible to probe the dynamics of highly excited atoms and molecules (*12*), but the enormous density of states in these energy regimes often makes it difficult to perform or interpret quantum calculations. By contrast, in these regimes classical methods may still be tractable (*3, 6, 13–20*). The most obvious classical approach is to integrate trajectories numerically and try to extract trends from the resulting data. However, even in a classical simulation, interpretation of the actual dynamics in high-energy regimes is fraught with difficulty because of the complexity of the motion and the mass of data that must be generated and interpreted in order to develop a global picture of the dynamics. A better approach is based on the use of classical perturbation theory, which can provide a geometrically appealing and comprehensive overall description of the classical behavior that often uncovers systematic trends buried in the otherwise complicated dynamics. This type of analysis also lends itself willingly to quantization by semiclassical approaches, thus allowing a connection to be made with quantum mechanics.

Semiclassical Mechanics

Semiclassical mechanics (*21–23*), an outgrowth of Bohr's theory, provides the link between classical and quantum dynamics. The basic idea is to impose quantization on various classical quantities in order to provide agreement with empirical observations. This was first done by Bohr for the hydrogen atom, where quantization of the angular momentum of the electron was postulated in order to account for the hydrogenic spectrum. A simpler example that is relevant to molecular structure is that of bound 1-D vibrational motion (a harmonic oscillator, for example) whose energy E can be quantized semiclassically by means of the modified Wilson-Sommerfeld condition,

$$J = \oint P(E, q)dp = \left(n + \frac{1}{2}\right)h \tag{1}$$

In Eq. 1 P and q are the conjugate momentum and position, the quantum number $n = 0, 1, 2, \ldots$, and J is a generalized momentum variable called the classical action (the generalized coordinate associated with the action is called an angle, best thought of as a phase). This formula establishes the close connection between classical actions and quantum numbers. The integral is over a single classical period and represents an implicit equation for the allowed (quantized) energies. Quantization of multidimensional separable systems is straightforward because there is one such condition for each degree of freedom. Although an N-dimensional system may be separable, most physically interesting systems are not. If N independent classical conserved quantities exist, then the problem is termed integrable and quantization can be accomplished by the use of a method developed by Einstein in 1917. This approach is referred to as Einstein-Bruillouin-Keller (EBK) quantization (*15, 16, 17, 24*) and is a generalization of Eq. 1. For vibrational motion the EBK rule is

$$\int_{C_i} \bar{P} \cdot \bar{q} = \left(n_i + \frac{1}{2}\right)h, i = 1, 2, \ldots N \tag{2}$$

giving rise to N quantization conditions, all of which must be satisfied simultaneously. The C_i are contours of integration, which are a set of N topologically independent paths on the surface of a torus having dimension N in the $2N$-dimensional phase-space. Figure 1 illustrates two such paths on a torus embedded in a 4-D phase-space corresponding to an integrable Hamiltonian system. Most interesting atomic and molecular problems feature Hamiltonians that are nonintegrable (chaotic) and Eq. 2 breaks down. The object of current research in this area is to develop semiclassical methods capable of treating multidimensional nonintegrable dynamics, building on the semiclassical techniques pioneered by Miller and co-workers (*21, 22*) and by Marcus and co-workers (*15*) [for reviews, see (*14–23*)]. Nevertheless, fundamental problems remain in the extension of these methods to nonintegrable dynamics. Even in the integrable case it may be unclear how to effect quantization if multidimensional tunneling is important.

Recent advances in the application of semiclassical theory to nonseparable dynamics have resulted from combining group theory with classical perturbation methods developed mainly in the context of celestial mechanics. An outstanding and historically important example of the use of classical perturbation theory was provided by Delaunay for the earth-moon-sun system (*3, 25*). He performed an extraordinarily tedious series of canonical transformations by hand to obtain a perturbation expansion approximating the actual Hamil-

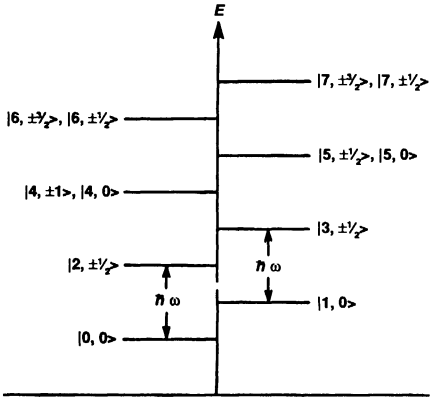

Fig. 2. Diagram illustrating the structure of the energy spectrum of a 2:1 anisotropic oscillator. It can be viewed as being made up of the energy levels of two 1:1 resonant isotropic oscillators with different zero point energies. The states are labeled $|n, r>$, where n is the total number of quanta and r quantizes the action J_2 in Eq. 7. Adapted from (*33*).

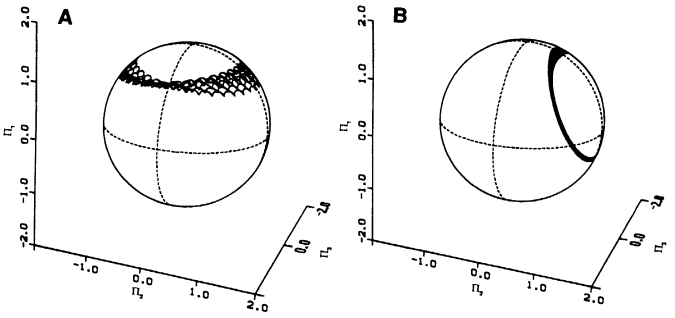

Fig. 3. Trace of trajectories for a model of the formaldehyde molecule on the vibrational constant energy sphere for two different values of the Coriolis coupling. In (**A**) there is relatively weak Coriolis coupling and the SU(2) generator π_1 (corresponding to the difference in energy between the modes, see Eq. 4) is preserved. In (**B**) the Coriolis coupling is stronger and π_1 is no longer a good constant of the motion, corresponding to extensive mode-mode energy transfer.

tonian and ultimately obtained good agreement with observations. In the language of modern-day nonlinear classical dynamics, the actual chaotic (nonintegrable) Hamiltonian is replaced by a nonchaotic (integrable) approximation that is designed to give good agreement with the real dynamics. This is a philosophy that is by no means outdated: The upsurge of interest in classical and celestial mechanics is due in large measure to modern-day successors of Delaunay such as Deprit and his colleagues (*26, 27*), who have developed efficient computer algebra programs to perform the necessary manipulations and equally sophisticated color graphics methods that provide significant new insights into the classical behavior. The level of success enjoyed by these approaches in terms of both accuracy and insight is quite spectacular. Deprit and co-workers have obtained very high order normal (integrable) approximations to problems of interest in celestial mechanics (*25*), the theory of artificial satellites (*26*), and atomic physics (*27*) [see also (*3, 4, 28*) for further details of the implementation of perturbation theory].

Once an approximate integrable Hamiltonian has been obtained, the energy can then be quantized semiclassically. In molecular physics the use of classical perturbation techniques [the Birkhoff-Gustavson normal form (BGNF) method] in semiclassical quantization was pioneered by Swimm and Delos (*29*), who quantized a simple nonresonant Hamiltonian designed to model vibrations in a triatomic molecule. However, their approach needed augmentation because it did not generate a complete energy spectrum when applied to a 1:1 resonant Hamiltonian (that is, a system with equal frequencies). Jaffé and Reinhardt (*30*) solved this problem by a different choice of unperturbed action-angle variables (polar rather than Cartesian). They were also able to calculate level splittings due to tunneling by using a uniform semiclassical quantization (*21–23*), which goes beyond the simple EBK rule. Despite early successes, however, it rapidly became clear that a more general approach had to be developed to treat the case of Fermi (or m:n) resonant systems (*31–33*). This issue was not addressed directly until fairly recently and concerns how to choose the best unperturbed action-angle variables in which to perform perturbation theory, effect quantization, and study the dynamics. The resolution of this problem has significant implications for both classical and semiclassical mechanics.

Many of the developments in the semiclassical theory of bound states have resulted from studies of perturbed harmonic oscillators, which may be used to model molecular vibrational modes. The unperturbed part of the Hamiltonian typically has the form

$$H = \frac{1}{2}(P_x^2 + P_y^2 + \omega_x^2 x^2 + \omega_y^2 y^2) \tag{3}$$

where it will be assumed for now that $\omega_x = 2\omega_y$ [the case for the anisotropic oscillator containing the famous 2:1 Fermi resonance of molecular physics (*31*)]. Figure 2 shows some of the low-lying levels of the Hamiltonian in a rather suggestive way. It is apparent that the energy levels can be broken up into two sets, each of which is in one-to-one correspondence with the eigenvalues of an isotropic oscillator (the two sets of levels correspond to those of two isotropic oscillators with different zero point energies). If the resonance is m:n, then the energy levels may be broken up into ($m \times n$) sets of isotropic oscillator levels. The degeneracy pattern is complicated, and in an application of degenerate quantum perturbation theory some care would have to be exercised in choosing appropriate basis functions. The situation is analogous in semiclassical mechanics where the unperturbed actions (or tori) must be chosen judiciously in order to avoid unphysical singularities in the limit of vanishing perturbation. The diagram in Fig. 2 implies that a study of the symmetry of the isotropic oscillator might shed light on the choice of the correct actions. In fact, extensive group theoretical analysis by a number of workers (*32*) shows that the symmetry of the 2:1 (or m:n) resonant 2-D oscillator is SU(2) just like the isotropic oscillator.

For the 1:1 isotropic oscillator,

$$H = \pi_0 = \frac{1}{2}(P_x^2 + P_y^2 + \omega^2 x^2 + \omega^2 y^2) \tag{4a}$$

there are three conserved classical quantities besides H itself,

$$\pi_1 = \frac{1}{2}(P_x^2 + \omega^2 x^2) - \frac{1}{2}(P_y^2 + \omega^2 y^2) \tag{4b}$$

$$\pi_2 = yP_x - xP_y \tag{4c}$$

$$\pi_3 = P_x P_y + xy \tag{4d}$$

which satisfy the same classical commutation (Poisson bracket) relations as angular momentum (to within a factor of 2)

$$\{\pi_j, \pi_k\} = 2\epsilon_{jk\ell}\pi_\ell \tag{5}$$

where $\epsilon_{jk\ell}$ is the Levi-Civita symbol for permutations of the indices (i, j, k): it is equal to 1 for even permutations and to -1 for odd permutations and is zero otherwise. Together with the relation

$$\pi_0^2 = \pi_1^2 + \pi_2^2 + \pi_3^2 \tag{6}$$

the π_i's (i = 1,2,3) generate an SU(2) Lie algebra. Equation 6 shows an interesting geometric property of these quantities. They define a constant-energy sphere (the Hopf sphere) whose radius is the unperturbed energy π_0. The other π's act like Cartesian coordinates on the surface of the sphere. Thus the isotropic oscillator orbits in 4-D phase-space may be mapped into points on the surface of the 3-D Hopf sphere. The same is true for a Fermi resonance but the generators have different and much more complicated functional forms, which can be obtained by the use of methods described elsewhere (*32, 33*). For the purposes of this article it is sufficient to note that the SU(2) symmetry is preserved for resonances other than 1:1 in two dimensions.

A problem in dealing with resonant systems is the nonuniqueness in the choice of unperturbed actions. However, the Lie algebraic approach described by Farrelly (*33*) explains how to construct an appropriate set of unperturbed actions in which to apply perturbation theory and subsequently effect quantization. The transformation to action-angle variables can be performed directly, and the beauty of the approach is that extensive and intricate canonical

transformations to switch between the different sets of unperturbed actions are avoided. In this case two unperturbed actions must be defined. J_1 (the principal action) defines the radius of the sphere and is conserved (its conjugate angle variable does not appear in a perturbation expansion). One possible transformation from SU(2) generators directly to action-angle variables is the following (*30, 33–35*),

$$\pi_0 = J_1$$
$$\pi_1 = \sqrt{J_1^2 - J_2^2}\cos 2\varphi_2$$
$$\pi_2 = J_2$$
$$\pi_3 = \sqrt{J_1^2 - J_2^2}\sin 2\varphi_2 \qquad (7)$$

The Lie algebraic approach is being used by several groups and is of considerable importance in both vibrational and rotational problems. In particular the idea of using the SU(2) sphere to portray phase-space has proved useful in analyzing the resonance structure of nonlinearly coupled oscillators (*34, 36*) (see Fig. 3). The commutation relations satisfied by the SU(2) generators also allow a connection to be made between vibrational problems in two dimensions and the asymmetric top (*36*). Harter (*34, 37*) has pointed out the connection between SU(2) generators and the theory of optical polarization ellipsometry as developed by Stokes 130 years ago. Another significant application in optics is by Holm and co-workers (*38*) in the study of chaos in nonlinear optical beams.

Rotational and Vibrational Dynamics

It is becoming apparent that rotational-vibrational interactions are of central importance to the dynamics of highly excited polyatomic molecules (*12*). In particular, studies of the role of rotation in intramolecular energy transfer have focused on the determination of good or almost good quantum numbers. Classically, these correspond to conserved or almost conserved classical actions. For example, the breakdown of the quantum number K, which quantizes the projection of the total molecular angular momentum onto a molecule-fixed axis, signals strong rotational-vibrational interactions in molecules such as formaldehyde, CH_2O. Several studies of CH_2O connect the breakdown of K to vibrations in the molecular frame, which may be modeled as a pair of nearly degenerate nonlinearly coupled modes (*39, 40*). Much of the analysis described in the previous section can be used to provide a compelling and informative picture of how energy flow proceeds in excited molecules in which rotational and vibrational energy transfer is occurring.

It is useful to begin with the asymmetric top, which is one of the simplest problems relevant to molecular rotations. This system also constitutes a basic paradigm for the applications that will be discussed in this article. The Hamiltonian for the torque-free motion of an asymmetric top may be written in terms of the body-fixed components of angular momentum (*41, 42*),

$$H = AJ_x^2 + BJ_y^2 + CJ_z^2 \qquad (8)$$

where A, B, and C are the rotational constants. Conservation of angular momentum requires that

$$\mathbf{J}^2 = J_x^2 + J_y^2 + J_z^2 \qquad (9)$$

Because $\mathbf{J}$ is an angular momentum, its components also generate an SU(2) Lie algebra. This allows the vibrational Hamiltonians of the previous section to be mapped onto the asymmetric top, and vice versa (*34, 40*). A superb way of visualizing the mechanics, which provides insight into the energy level structure, was invented by Harter and Patterson (*41*) and consists of constructing a rotational energy surface (RES) for the problem using the generators of the Lie algebra. An RES is a plot of total energy as a function of the direction of an angular momentum vector (in a body-fixed frame) for a constant value of $|\mathbf{J}|$ (*41, 42*). The components of angular momentum are interpreted as Cartesian coordinates of a position vector whose length is given by H, which is plotted radially outward. The rotational energy surface will be used in the consideration of the hydrogen atom in external fields described in the next section, which can also, in certain cases, be represented as a 2-D oscillator. An example of an RES for an asymmetric top is shown in Fig. 4. The contours on the surface represent the intersection of spheres (whose radii are the total energy) with the rotational energy surface. For the asymmetric top there are two types of energy state corresponding to librational and rotational motion. In Fig. 4 the two topologically different kinds of state are clearly visible on the RES, as is the separatrix between them (*41*). Also shown in Fig. 4 is a path along which tunneling occurs, lifting the degeneracy between the vibrational states.

A good example of the appeal of classical techniques in discussing intramolecular dynamics is provided by the CH_2O molecule. Stimulated emission pumping experiments by Dai *et al.* (*43*) imply that rotation-vibration coupling is a major way in which intramolecular energy flow occurs, even for moderate values of the total angular momentum. Although CH_2O is a fairly simple molecule, the existence of very strong mode-mode coupling means that the general problem of intramolecular energy flow cannot be treated in any simple way. However, in certain energy regimes it is possible to construct a simple model Hamiltonian that provides a reasonably good approximation to the vibrational and rotational dynamics. The molecular Hamiltonian is approximated as two coupled vibrations (out-of-plane bending and the HCO wagging) and molecular rotation. As noted, an attractive geometrical way to portray the dynamics (*39, 40*) is to plot the trajectories on the SU(2) sphere. Figure 3 shows the trace of a trajectory on the vibrational constant energy sphere for weak and strong Coriolis couplings. For weak Coriolis coupling there is minimal vibrational energy flow, whereas for the higher Coriolis coupling energy flow is much more pronounced between the two vibrational modes. This simple geometrical analysis provides a way of understanding the breakdown of conserved quantities as a route to chaos as well as explaining the role of the various couplings in mediating energy flow.

Phase-space analysis of the CH_2O molecule reveals a strong similarity between it and the famous Lipkin-Meshkov-Glick (LMG) model of nuclear physics (*44*). The LMG Hamiltonian is a collective particle model consisting of N spins, and the unperturbed part of the LMG model corresponds to an asymmetric top. The connection with CH_2O has been exploited to treat the LMG model classically as

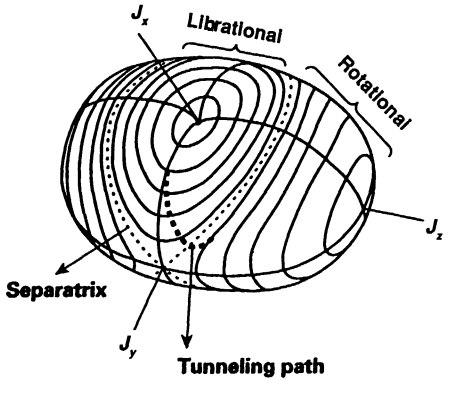

Fig. 4. Rotational energy surface for the asymmetric top. The contours are level curves of equal energy obtained by intersecting the RES with spheres of progressively greater energy. The librational (vibrational) and rotational states are indicated as is the classical separatrix between them. Also shown is a possible tunneling path between the otherwise degenerate librational states. Adapted from (*41*).

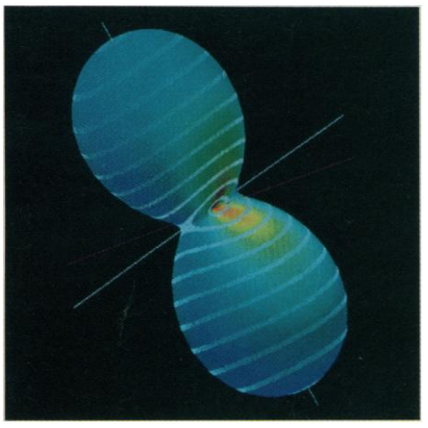

Fig. 5. Rotational energy surface for the QZE where the principal hydrogenic quantum number $n = 30$ and the magnetic field (γ) is 1.26×10^{-6} atomic unit (1 atomic unit = 2.35×10^5 T). The quasi-Landau (localized around the lobes) and Landau states (confined to the dimples) are clearly visible. The contours have the same meaning as in Fig. 4. Each RES has been pseudocolored (*26*) to indicate the absolute value of the "apt" classical action as a function of its conjugate phase angle ϕ as measured around the z axis (the z axis is colored red) (*32*): the color scale goes from blue (low) to red (high) (*52*).

well as to explain aspects of the rotational-vibrational dynamics of CH_2O itself (*40*).

Electronic Structure of Rydberg Atoms

In view of the relatively heavy effective masses involved, the treatment of molecular rotations and vibrations by classical and semiclassical methods might appear reasonable. It is perhaps more surprising that, in certain cases, classical approaches can be used to study the electronic structure of atoms. Although it would be unphysical to expect that any method could follow the actual dynamics of an electron, semiclassical methods can and do provide an accurate description of the electronic level structure of atomic Rydberg states. Far from being a solved problem, the interaction of the hydrogen atom with external fields has become a unique atomic laboratory for the study of chaos. In 1980 Zimmerman, Kash, and Kleppner (*45*) proposed that the hydrogen atom in a strong magnetic field [the quadratic Zeeman effect (QZE)] has a hidden symmetry. This proposal marked the start of a decade of extraordinary theoretical and experimental interest in this and related problems (*3, 5, 6, 13, 47, 48*). Activity is continuing, and recent experiments by Kleppner and co-workers have also revealed the existence of orderly progressions in the spectra of Li atoms in strong magnetic fields (*46*). This order is so remarkable because it is found in a regime in which the classical motion is strongly chaotic.

Many studies of the QZE have been concerned primarily with understanding the chaotic nature of the dynamics (*3, 6, 13, 47*). The external fields break the symmetry, and it is this symmetry breaking that gives rise to nonintegrability in the system. Although dynamical symmetry breaking as a route to chaos is quite well understood in purely classical systems, much less can be said in the case of quantum systems (*3, 5, 6*). From the point of view of understanding the interaction of fields with Rydberg states and their spectroscopy, partially broken or approximate symmetries can often be used to provide important insight into the physics. Quite apart from considerations related to nonlinear dynamics and chaos, Rydberg states in external fields are of significant interest in their own right: an important and technologically relevant example from solid-state physics is the interaction of excitonic states with external electromagnetic fields.

For the QZE through second order in the magnetic field, the "hidden" dynamical constant of motion is (*45, 49, 50*)

$$\Lambda = 4\mathbf{A}^2 - 5\mathbf{A}_z^2 \tag{10}$$

where $\mathbf{A}$ is the Laplace-Runge-Lenz vector and Λ lies in the range $-1 \leq \Lambda \leq 4$. Classically the Laplace-Runge-Lenz vector is a constant of the motion that is in the direction of the radius vector to the perihelion of the orbit and is responsible for the closure of the Kepler orbit. The quantum operator corresponding to this quantity accounts for the extra degeneracy in the hydrogen atom (*49*).

In cylindrical coordinates and atomic units ($m = e = \hbar = 1$, where m is mass and e is electronic charge) the QZE is 2-D, with Hamiltonian

$$H = E = \frac{1}{2}(P_\rho^2 + P_z^2) + \frac{P_\phi^2}{2\rho^2} + \frac{1}{8}\gamma^2\rho^2 - \frac{1}{\sqrt{(\rho^2 + z^2)}} \tag{11}$$

where P is momentum, $\rho = \sqrt{x^2 + y^2}$, and the reduced field, $\gamma = B/(2.35 \times 10^5$ T), where B is the external magnetic field. The discussion is simplified if only the $m = 0$ ($P_\phi = m\hbar = 0$) case, which

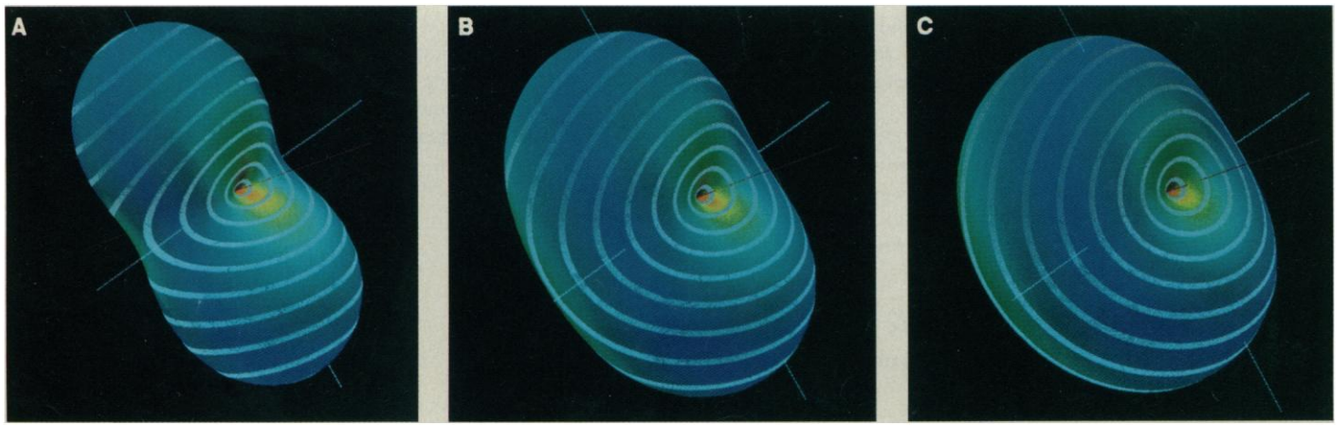

Fig. 6. A series of rotational energy surfaces for the SQZE where the principal hydrogenic quantum number $n = 30$. The contours have the same meaning as in Fig. 4. The magnetic field (γ) is 1.26×10^{-6} atomic unit in all frames and the electric field (F) is being progressively increased. The perturbation strength is defined by $\beta = (4/25)\ F/(n\gamma^2)$ (*56*). The surfaces have been pseudocolored according to the scheme described in Fig. 5. The librational states are localized in the dimples (see Fig. 5), which appear red, indicating high absolute values of the action. The case for $\beta = 0$ (the pure QZE) is shown in Fig. 5. In (**A**) $\beta = 0.2$ and one class of librational state has vanished (not visible) while the other has grown. The librational states continue to take over as the electric field increases as is evident in (**B**) where $\beta = 0.5$. In (**C**) $\beta = 1.0$, the rotational states have completely disappeared, and only a single class of librational states exists. At this high field the variation of the action with ϕ is minimal, indicating its approximate conservation.

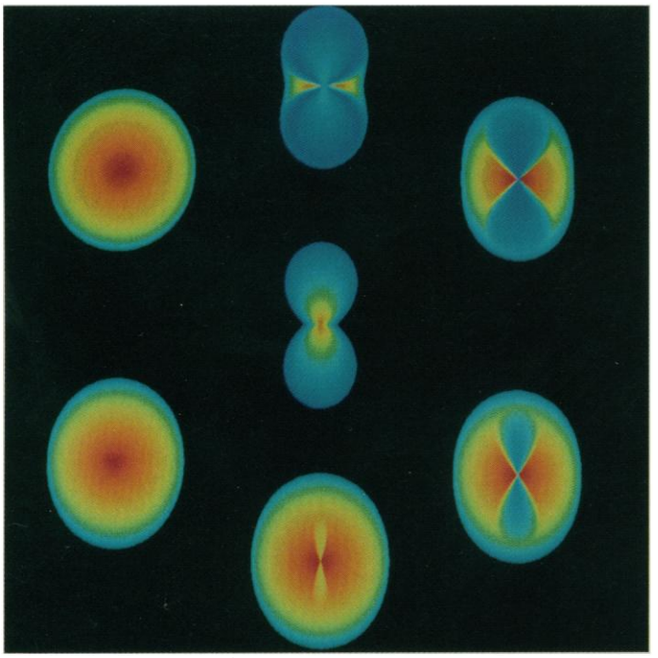

Fig. 7. A global view of the transition of the RES on going from the pure QZE to a case that is almost the pure Stark effect. The energy contours have been omitted, and the RES is viewed from behind as compared to Fig. 6. The surfaces have been pseudocolored according to the scheme described in Fig. 5, and the perturbation parameters are as in Fig. 6. The pure QZE ($\beta = 0$) is shown in the center. The image at 12 o'clock has $\beta = 0.2$. If we continue clockwise, the electric field is increased according to the sequence: $\beta = 0.5$, 0.7, 0.9, 1.0, and 2.0. The disappearance of a class of librational states at $\beta = 0.2$ and the rotational states at $\beta = 1.0$ is readily apparent.

has been the subject of most experimental studies and is representative of the dynamics for all m, is considered. If we use a transformation from celestial mechanics, the singularity can be avoided by going over to "regularized" parabolic coordinates u, v (*50, 51*), which make the SU(2) symmetry of the system apparent and facilitate application of classical perturbation theory. The $m = 0$ Hamiltonian becomes (*50, 51*)

$$\mathcal{H} = \frac{2}{\sqrt{-2E}} = \frac{1}{2}(P_u^2 + u^2) + \frac{1}{2}(P_v^2 + v^2) + \frac{\gamma^2}{32E^2}(u^2 + v^2)u^2v^2 \tag{12}$$

Interestingly, this Hamiltonian resembles a problem in molecular vibrations where the coupling depends on the strength of the applied field. BGNF theory provides an integrable approximation (the normal form) to $\mathcal{H}_{NF}$ which can be written in terms of the SU(2) generators. To order γ^2 it is

$$\mathcal{H}_{NF} = \pi_0 + \lambda\pi_0[5(\pi_0^2 - \pi_1^2) - 4\pi_2^2] \tag{13}$$

where the π's have the same meaning as in Eq. 4 (if the Cartesian coordinates are replaced by regularized coordinates) and λ depends on the magnetic field quadratically.

One can map the QZE onto an asymmetric top by using Eq. 13 and interpreting the SU(2) generators as the components of a generalized angular momentum (*52–54*). Doing so allows an RES to be constructed as displayed in Fig. 5. The low-energy vibrational or librational (Landau) and higher energy rotational (quasi-Landau) states are seen to be separated by the classical separatrix. The Landau states are located in either dimple of the RES, and tunneling between these dimples lifts the degeneracy of the states. The high-lying localized quasi-Landau (rotor) states are confined to the extended lobes of the RES (*53*) and correspond to the ridge states of Fano (*52, 55*). Obtaining the correct geometrical picture is important for the success of semiclassical calculations of energy levels themselves. Quantization of the classical perturbation expansion obtained with Lie algebraic methods gives outstanding agreement with quantum results, even reproducing all of the splittings due to tunneling on the RES (*52*). Although application has only been described for the $m = 0$ case, which has SU(2) symmetry, the full QZE may be treated as an SU(2) × SU(2) problem in a similar fashion, and this also provides good agreement with quantum results.

A related problem of experimental (*56*) and theoretical (*57*) interest is the QZE in the presence of a weak electric field [the Stark-QZE (SQZE)]. Addition of a weak electric field parallel to the magnetic field direction does not break the approximate SU(2) symmetry but does result in more complicated dynamics. By performing BGNF theory for the SQZE Hamiltonian to second order in the magnetic field and to first order in the electric field, RES's may be constructed as shown in Fig. 6 as a function of increasing electric field. The sequence of RES's in Fig. 6 illustrates the major changes that occur as the electric field is increased. The symmetry between the librational states in the pure QZE is broken for nonzero values of the electric field resulting in three classes of state (two librational classes, localized in the dimples of the RES and a rotational class of states): as the electric field is increased, one class of librational levels disappears, followed by the disappearance of the rotational states. Eventually only a single class of librational states persists (*56*). This manifests itself in Fig. 6 by the gradual growth of the states around one of the red dimples and the eventual merging of the two lobes of the RES. The best classical action variable to quantize is the same as for the QZE as described by Farrelly and Krantzman (*52*). The RES's in Fig. 6 have been pseudocolored to reflect the value of this action variable as a function of its conjugate angle, ϕ, which is the azimuthal angle around the z axis. The variation in the action is found by tracing ϕ along contours of equal energy on the RES. At low electric fields there is substantial variation in the action as a function of ϕ. As the electric field is increased this variation decreases, indicating that the action is progressively becoming a better constant of motion [in the absence of the magnetic field it is an exact constant (*58*)]. Figure 7, which provides an alternative view of the RES's, gives a clear and accurate description of this process.

These recent developments in the study of the QZE provide an outstanding example of how classical and semiclassical methods can provide qualitative and quantitative insight into dynamical systems. Most initial theoretical studies of the QZE were large-scale quantum calculations that reproduced experimental observations fairly well and confirmed the existence of an approximate symmetry. However, as illustrated in a series of three recent publications by Farrelly and Krantzman (*52*), Uzer (*53*), and Rau and Zhang (*54*), all this information is contained in simple classical and semiclassical models, which provide a simple interpretation of trends buried in the apparently complicated dynamics.

Conclusions

The application of classical mechanics to essentially quantum systems has a long history, and it appears that classical methods will continue to be applied successfully to problems in atomic, molecular, and nuclear physics. Combining nonlinear dynamics, group theory, and semiclassical methods provides a powerful way of determining the underlying structure and trends in either experimental data or detailed numerical simulations. For several examples chosen from microscopic physics, a simple picture emerged that

unified and clarified the results of a large number of experimental, quantum, and even classical studies. A number of issues remain, however, including the treatment of more than two dimensions where phenomena such as Arnold diffusion (*4*) may be important, and the correspondence principle limit of quantum mechanics (*3, 5*) when the classical dynamics is chaotic. Nevertheless, it is likely that the approaches briefly overviewed in this article will continue to be of widespread utility in interpreting the ever-increasing amounts of experimental and computational data that are becoming available to chemists and physicists.

REFERENCES AND NOTES

1. M. Born, *Mechanics of the Atom* (republished by F. Ungar, New York, 1960)(translated by J. W. Fisher).
2. I. C. Percival, *Proc. R. Soc. London Ser. A* **353**, 289 (1977): R. S. Berry, *Contemp. Phys.* **30**, 1 (1989).
3. An outstanding detailed overview of the field is given by M. C. Gutzwiller, *Chaos in Classical and Quantum Mechanics* (Springer-Verlag, New York, 1990).
4. A. J. Lichtenberg and M. A. Lieberman, *Regular and Stochastic Motion* (Springer-Verlag, New York, 1983).
5. H. Flaschka and B. V. Chirikov, Eds., *Progress in Chaotic Dynamics: Essays in Honor of Joseph Ford's 60th Birthday* (North-Holland, Amsterdam, 1988).
6. T. Grozdanov, P. Grujić, P. Krstić, Eds., *Proceedings of the International Conference on Chaotic Dynamics in Atomic and Molecular Physics* (World-Scientific, Singapore, 1989); B. Eckhardt, *Phys. Rep.* **163**, 205 (1988).
7. S. Califano, *Vibrational States* (Wiley, London, 1976).
8. J. Ford, in *The New Physics*, P. Davies, Ed. (Cambridge Univ. Press, Cambridge, U.K., 1989), pp. 348–371; G. H. Walker and J. Ford, *Phys. Rev.* **188**, 416 (1969).
9. J. Wisdom, S. J. Peale, F. Mignard, *Icarus* **58**, 137 (1984): L. M. Polvani, J. Wisdom, E. DeJong, A. P. Ingersoll, *Science* **249**, 1393 (1990).
10. G. Casati, B. V. Chirikov, J. Ford, F. M. Izrailev, *Lec. Notes Phys.* **93**, 334 (1979): for a review, see F. M. Izrailev, *Phys. Rep.* **196**, 299 (1990).
11. M. Duncan, T. Quinn, S. Tremaine, *Icarus* **82**, 402 (1989).
12. For a recent review, see T. Uzer, *Phys. Rep.* **199**, 73 (1991). The entire issue of *J. Opt. Soc. Am. B* 7, 1801–1979 (1990) is devoted to the area of molecular spectroscopy and dynamics as probed by stimulated emission pumping.
13. G. F. Bassani, M. Inguscio, T. W. Hänsch, Eds., *The Hydrogen Atom* (Springer-Verlag, Berlin, 1989).
14. N. C. Handy, in *Semiclassical Methods in Scattering and Spectroscopy*, M. S. Child, Ed. (Reidel, Dordrecht, 1980), pp. 297–321.
15. D. W. Noid, M. L. Koszykowski, R. A. Marcus, *Annu. Rev. Phys. Chem.* **32**, 267 (1981).
16. W. P. Reinhardt, in *Chaotic Behavior in Quantum Systems: Theory and Applications*, G. Casati, Ed. (Plenum, New York, 1985), p. 235.
17. J. B. Delos and M. L. Du, *IEEE J. Quantum Electron.* **24**, 1445 (1988).
18. E. J. Heller and E. B. Stechel, *Annu. Rev. Phys. Chem.* **35**, 563 (1984).
19. G. S. Ezra, C. C. Martens, L. E. Fried, *J. Phys. Chem.* **91**, 3721 (1987).
20. W. P. Reinhardt, *Adv. Chem. Phys.* **73**, 925 (1989).
21. W. H. Miller, *ibid.* **25**, 69 (1974); S. Chapman, B. C. Garrett, W. H. Miller, *J. Chem. Phys.* **64**, 502 (1976).
22. W. H. Miller, *Science* **233**, 171 (1986).
23. M. V. Berry and K. E. Mount, *Rep. Prog. Phys.* **35**, 315 (1972).
24. See (*3*), p. 151.
25. C. Delaunay, *Theorie du Mouvement de la Lune*, premier volume, *Mém. Acad. Sci. Paris* **28** (1860); *ibid.*, second volume, **29** (1867). Several errors in Delaunay's results were pointed out by A. Deprit, J. Henrard, and A. Rom [*Astron. J.* **76**, 269 (1971)]. See also an article by R. Pavelle, M. Rothstein, and J. Fitch on the usefulness of computer algebra methods in this context [*Sci. Am.* **245**, 136 (December 1981)].
26. S. Coffey, A. Deprit, E. Deprit, L. Healy, *Science* **247**, 833 (1990). See the cover of that issue for a remarkable example of the power of pseudocoloring to uncover details of the dynamics.
27. S. L. Coffey, A. Deprit, B. Miller, C. A. Williams, *Ann. N.Y. Acad. Sci.* **497**, 22 (1987).
28. J. Cary, *Phys. Rep.* **79**, 129 (1981); M. A. Olshanetsky and A. M. Perelomov, *ibid.* **71**, 313 (1981); *ibid.* **94**, 313 (1983).
29. R. T. Swimm and J. B. Delos, *J. Chem. Phys.* **71**, 1706 (1979).
30. C. Jaffé and W. P. Reinhardt, *ibid.*, p. 1862.
31. E. Fermi, *Z. Phys.* **71**, 250 (1931).
32. V. A. Dulock and H. V. McIntosh, *Am. J. Phys.* **33**, 109 (1965); H. V. McIntosh, *ibid.* **27**, 620 (1959): A. Cisneros and H. V. McIntosh, *J. Math. Phys. (N.Y.)* **11**, 870 (1970); G. A. Baker, *Phys. Rev.* **103**, 1119 (1956).
33. D. Farrelly, *J. Chem. Phys.* **85**, 2119 (1986).
34. W. G. Harter, *ibid.*, p. 5560.
35. The particular choice of J_2 is critical and specific to the perturbation (*33, 34*) but is obtainable by permuting the subscripts on π_1, π_2, and π_3 in Eq. 7, equivalent to a rotation on the Hopf sphere. In the *m*:*n* resonant anisotropic case the apt actions in which to perform perturbation theory will also be expressible in terms of the SU(2) generators. The functional forms of the generators differ depending on the unperturbed resonance but they are expressible in terms of the classical equivalent of boson operators. Once determined, the transformation to action-angle variables is the same as in Eq. 7. This is similar to Schwinger's picture of angular momentum where the SU(2) generators can be identified with the angular momentum components J_x, J_y, and J_z [J. Schwinger, *On Angular Momentum*, Atomic Energy Commission Rep. NYO-3071 (1952)].
36. D. K. Sahm and T. Uzer, *J. Chem. Phys.* **90**, 3159 (1989); D. K. Sahm, S. McWhorter, T. Uzer, *ibid.* **91**, 219 (1989): L. Xiao and M. E. Kellman, *ibid.* **90**, 6086 (1989).
37. Original references for the theory of optical polarization are: G. Stokes, *Proc. R. Soc. London* **11**, 545 (1862): H. Poincaré, *Theorie Mathematique de le Lumière* (Gauthieres Villars, Paris, 1892). A color animation computer program to visualize the dynamics of oscillator motion and display interactively the parameters for optical polarization ellipsometry has been developed by Harter (Earthings Co., c/o W. G. Harter, Department of Physics, University of Arkansas, Fayetteville, 72701). See also W. G. Harter and N. dos Santos, *Am. J. Phys.* **46**, 251 (1978).
38. D. David, D. D. Holm, M. V. Tratinik, *Phys. Lett. A* **137**, 355 (1989); *ibid.* **138**, 29 (1989); *Phys. Rep.* **187**, 281 (1990).
39. S. K. Gray and M. J. Davis, *J. Chem. Phys.* **90**, 5420 (1989); M. Aoyagi and S. K. Gray, *ibid.* **94**, 195 (1991); D. C. Burleigh, R. C. Mayrhofer, E. L. Sibert III, *ibid.* **89**, 7201 (1988).
40. D. K. Sahm, R. V. Weaver, T. Uzer, *J. Opt. Soc. Am.* **7**, 1865 (1990).
41. W. G. Harter and C. W. Patterson, *J. Chem. Phys.* **80**, 4241 (1984); W. G. Harter, *J. Stat. Phys.* **36**, 749 (1984); *Comput. Phys. Rep.* **8**, 319 (1988).
42. R. N. Zare, *Angular Momentum: Understanding Spatial Aspects in Chemistry and Physics* (Wiley, New York, 1988).
43. H.-L. Dai, C. L. Korpa, J. L. Kinsey, R. W. Field, *J. Chem. Phys.* **82**, 1688 (1985).
44. H. J. Lipkin, N. Meshkov, A. J. Glick, *Nucl. Phys.* **62**, 188 (1965).
45. M. L. Zimmerman, M. L. Kash, D. Kleppner, *Phys. Rev. Lett* **45**, 1092 (1980).
46. C. Iu, G. R. Welch, M. L. Kash, L. Hsu, D. Kleppner, *ibid.* **63**, 1133 (1989).
47. For recent reviews, see: J. C. Gay, in *Atoms in Unusual Situations*, J. P. Briand, Ed. (Proceedings of the North Atlantic Treaty Organization Advanced Study Institutes, Series B, Physics, Plenum, New York, 1986), vol. 143, p. 1073; H. Hasegawa, M. Robnik, G. Wunner, *Prog. Theor. Phys. Suppl.* **98**, 198 (1989); H. Friedrich and D. Wintgen, *Phys. Rep.* **183**, 37 (1989).
48. A. Holle, J. Main, G. Wiebusch, H. Rottke, K. H. Welge, *Phys. Rev. Lett.* **61**, 161 (1987).
49. E. A. Solv'ev, *Sov. Phys. JETP Lett.* **34**, 265 (1981); *Sov. Phys. JETP* **55**, 1017 (1982); D. R. Herrick, *Phys. Rev. A* **26**, 323 (1982). An independent determination of Λ for the case $m = 0$ was obtained by Reinhardt and Farrelly (*50*). The invariant Λ is a consequence of the approximate separability of the QZE through second order in the magnetic field in elliptical cylindrical coordinates on the O(4) sphere. See also Y. Alhassid, E. A. Hinds, and D. Meschede [*Phys. Rev. Lett.* **59**, 1545 (1987)]. An interesting account of the Laplace-Runge-Lenz vector is given by H. Goldstein in *Am. J. Phys.* **44**, 1123 (1976).
50. W. P. Reinhardt and D. Farrelly, *J. Phys. (Paris) Colloq.* **43**, C2 (1982).
51. A. R. Edmonds and R. A. Pullen, Imperial College preprint ICTP (79–80), p. 28.
52. D. Farrelly and K. Krantzman, *Phys. Rev. A* **43**, 1666 (1991).
53. T. Uzer, *ibid.* **42**, 5787 (1990).
54. A. R. P. Rau and L. Zhang, *ibid.*, p. 6342.
55. U. Fano, F. Robicheaux, A. R. P. Rau, *ibid.* **37**, 3655 (1988).
56. P. Cacciani, S. Liberman, E. Luc-Koenig, J. Pinard, C. Thomas, *J. Phys. B* **21**, 3473 (1988); *ibid.*, p. 3499; *ibid.*, p. 3523.
57. R. L. Waterland, J. B. Delos, M. L. Du, *Phys. Rev. A* **35**, 5064 (1987).
58. D. Farrelly and W. P. Reinhardt, *J. Phys. B* **16**, 2103 (1983).

59. Supported by the National Science Foundation and the Defense Advanced Research Projects Agency. We have benefited from discussions with J. L. Wood, K. D. Krantzman, and J. A. Griffiths.